

1 **Atmospheric Water Vapor Budget and its Long-term Trend over the Tibetan Plateau**
2

3 **Hongru Yan¹, Jianping Huang^{1*}, Yongli He¹, Yuzhi Liu¹, Tianhe Wang¹ and Jiming Li¹**

4 ¹Key Laboratory for Semi-Arid Climate Change of the Ministry of Education, College of
5 Atmospheric Sciences, Lanzhou University, Lanzhou 730000, China

6 Corresponding author: Jianping Huang (hjp@lzu.edu.cn)

7 **Key Points:**

- 8 • Although air of Tibetan Plateau are moistening, atmospheric water supply could not well
9 alleviate the depletion of surface water storage.
- 10 • Characteristics of water vapor balance vary from place to place across the Tibetan
11 Plateau, key areas refer to several basins.
- 12 • Regions around Yarlung Zangbo Grand Canyon suffer severe loss of water storage due to
13 overwhelming decrease in water vapor convergence.
- 14 • The source region of the Three Rivers also undertakes some risk to the depletion of
15 surface water storage.
16

17 Abstract

18 As rapid warming and consequent glaciers retreat across the Tibetan Plateau (TP), the problem
19 about whether or not atmospheric water supply could alleviate the depletion of surface water
20 storage need to be examined. Long-term changes of atmospheric water vapor balance across the
21 TP is investigated by the ERA5 reanalysis from 1979 to 2018. Annual accumulated precipitation,
22 water vapor convergence and evaporation generally keep an equilibrium but with different long-
23 term variation trends: 0.68mm/a, 0.68mm/a and -0.18mm/a, respectively. Results suggest that
24 surface water storage will not be well replenished by the water vapor transported from outside of
25 the TP. For different regions of the TP, characteristic of water vapor balance and their long-term
26 trends are completely different. Regions around Yarlung Zangbo Grand Canyon experiences
27 sharp decrease in water vapor convergence and leads to decrease in precipitation. Meanwhile,
28 evaporation keeps increasing due to the warming and melting of glaciers. Loss of surface water
29 storage should be severe. For the source region of the Three Rivers, decrease in water vapor
30 convergence overlaps increase in evaporations leads to no significant changes in total
31 precipitations. Decrease in water transported from outsides brings risk to the depletion of surface
32 water storage. Brahmaputra basin, inner TP and Qilian Mountain show significant wetting trends
33 due to the increases in both convergence of water vapor flux and evaporation. Above regional
34 characteristics of water vapor balances across the TP cause by inhomogeneous variation of
35 atmospheric heat source and changes of atmospheric circulations, which need to be studied in
36 further.

37 Plain Language Summary

38 By analyzing the long-term trends of precipitation, water vapor convergence and evaporation, we
39 try to estimate that whether the increase of atmospheric water vapor could replenish the depletion
40 of surface water storage across the Tibetan Plateau (TP). Results suggest that surface water
41 storage will not be overall replenished by precipitation for the whole year, because water vapor
42 from local evaporation is increase but from outside of the TP is decrease. Meanwhile, long-term
43 trends of water vapor balance and their consequent impacts on surface water storage vary from
44 place to place across the TP.

45 1 Introduction

46 The Tibetan Plateau (TP), which has an area of 2.5 million km² and average elevation of over
47 4000 m, is the highest and most extensive plateau in the world. It serves as the “world water
48 tower” storing large amounts of water as glaciers, lakes, and rivers ([Lu et al., 2005](#); [Yao et al., 2012](#)).
49 Seasonal melting of snowpack and mountain glaciers over the TP feeds seven major
50 rivers in Asia, providing abundant fresh water to about 40% of the world's population in this
51 region and its downstream areas. Due to its unique terrain and specific underlying surfaces, the
52 TP is well recognized to exert a dramatic influence on regional and even global climate ([Wu et al., 2012a](#);
53 [Ma et al., 2017](#)). Therefore, studying the atmospheric water over the TP is critical in
54 climate research and adaptation policy.

55 Due to Plateau “heat pump effect” ([Wu & Zhang, 1998](#)), TP can converge water vapor from
56 surrounding oceans or seas ([An et al., 2001](#); [Boo & Kuang, 2010](#); [Molnar et al., 1993](#); [Wu et al., 2007, 2012b](#)),
57 and becomes an isolated region of humidity in the atmosphere ([Xu et al., 2008a](#)).
58 The TP plays significant role in adjusting the atmospheric circulation and hydrological cycle.
59 Moreover, the TP is often considered as a “wet pool” and “transfer station” of the east Asian

60 moisture during summer (*Wang et al. 2011*) and to influence the precipitation over downstream
61 regions (*Wan et al. 2017; Xu et al. 2008b*) by transporting the water vapor by the westerly wind
62 and southwest monsoon (*Ding & Chan, 2005*). Meanwhile, the TP snow cover associated with
63 moisture anomaly have great impacts on East Asian atmospheric circulation (*Li et al., 2018,*
64 *2019*). Therefore, it is meaningful to understand the water vapor transport from the TP, one of
65 the most active centers of hydrological cycle in the world, and the further impact on the regional
66 weather and climate.

67 It was reported that, under climate mean conditions, TP is a moisture sink in summer, having
68 a net moisture convergence of 4 mm/day (*Feng & Zhou, 2012*). On a diurnal scale, *Ueno et al.*
69 (*2008*) found a strong daytime wind speed accompanied by increasing relative humidity prevails
70 along deep valleys in the Himalayas. However, the water vapor stagnates in front of the
71 Himalayas because of the southerly wind with weaker intensity (*Ueno et al., 2008*). Seasonally,
72 it was found that the passing of synoptic trough is expected to contribute strongly to water vapor
73 transport from the Indian Ocean to the TP during the monsoon season (*Sugimoto et al., 2008*).
74 On a long-term scale, it was reported that the precipitable water in the 680–310 hPa layer of the
75 atmosphere has increased significantly since the 1990s, with an upward trend of 6.45 cm per
76 decade and particularly high increases in summer (*Zhang et al., 2013*).

77 TP experienced a rapid warming over the past 50 years with two times more than the global
78 warming rates (*e.g. Liu & Chen, 2000; Guo & Wang, 2012*). Along with the climate changes, the
79 atmospheric circulation and hydrological cycles must be changed and the local environments
80 would be reshaped. Accompanying the warming, air over the TP moistened (*Xu et al., 2008a*),
81 surface pressure increased significantly (*Moore, 2012*), and surface heating and atmospheric
82 heating became weakened (*Zhu et al., 2008; Duan & Wu, 2008, 2009; Yang et al., 2011a,*
83 *2011b*), the wind speed showed a weakening trend (*Lin et al., 2013*). Furthermore, the surface
84 warming depends on elevation (*Liu & Chen, 2000*) and leads to glacier retreat, permafrost
85 degradation (*Cheng & Wu, 2007*), lake expansion (*Zhu et al., 2010*), runoff increase (*Lutz et al.,*
86 *2014*) and associated disaster risks aggravation (*Yao et al., 2012, 2019*). *Deng et al. (2018)* found
87 the terrestrial water storage over the TP increased by 0.20 mm/month during the 2002–2012
88 period, but decreased by –0.68 mm/month since 2012. In addition, *Immerzeel et al. (2010)*
89 projected that the warming may lead to less water resources for the downstream regions in the
90 future.

91 Combined all these facts, it is urgent to answer following questions: How do every
92 components of atmospheric water vapor budget generally vary on the inter-decadal time scale
93 across the TP? What factors are responsible for such inter-decadal variations? Could the
94 increasing of atmospheric water resources alleviate the depletion of terrestrial water storage
95 caused by the melting of glaciers and the increase of runoff? Answers to these questions could
96 enhance our understanding about inter-decadal variability of water vapor budget over the TP in
97 recent decades and the intrinsic mechanisms, and provide an evidence of the significance of
98 atmospheric water tower in the hydrological cycle on regional and global scales.

99 In this study, we focus on above questions to present a complete knowledge of atmospheric
100 water resources over the TP. First, we analyze climatology of atmospheric water vapor over the
101 TP based on ERA5 reanalysis data. Second, we examine climatology and long-term variations of
102 every components of water vapor budgets (water vapor transportation, evaporation and
103 precipitation) and give their related dynamical explanation. Finally, atmospheric water balance
104 over the TP has been discussed and summarized. Section 2 describes the data and accuracy of

105 each parameters used in this study. Section 3 presents the results and detailed discussions and
106 Section 4 presents the conclusions.

107 **2 Data**

108 ERA5 is the fifth generation European Centre for Medium-Range Weather Forecasts
109 (ECMWF) atmospheric reanalysis for the global climate and weather for the past 4 to 7 decades,
110 which is a replacement of ERA-Interim reanalysis. It has published a detailed record of the
111 evolution of the global atmosphere from 1979 to update and will be from 1950 onwards when
112 complete (*Berrisford et al., 2009; Dee et al., 2011*). Based on the 4D-Var assimilation method,
113 ERA5 provides estimates for each hour of the day, worldwide. The native resolution of the
114 ERA5 atmosphere and land reanalysis is 31km on a reduced Gaussian grid (T1639) and 63km
115 (TL319) for the ensemble members. The atmospheric component consists of 137 levels in the
116 vertical from the surface up to 1 Pa (about 80km). This spans the troposphere, stratosphere and
117 mesosphere. Data has been regridded to a regular lat-lon grid of 0.25 degrees for the reanalysis.
118 There are two main sub sets: data on pressure levels and data on single levels. The data on
119 pressure levels contain 16 atmospheric quantities on 37 pressure levels from 1000 hPa (surface)
120 to 1 hPa (around the top of the stratosphere). Single-level data are available for a number of
121 atmospheric, ocean-wave and land surface quantities. Information about the current status of
122 ERA5 production, availability of data online, and near-real-time updates of various climate
123 indicators derived from ERA5 data, can be found at <http://www.ecmwf.int/research/era>. Herein,
124 following parameters: total column water, specific humidity, vertical integral water vapor flux,
125 vertical integral moisture divergence, evaporation, snow evaporation and precipitation from
126 ERA5 monthly dataset have been applied to study the atmospheric water tower over Tibet
127 Plateau.

128 Care was needed when using reanalysis dataset to investigate trends of water vapor,
129 precipitation and evaporation over the TP due to their qualities. *Wang et al. (2017)* and *Zhao and*
130 *Zhou (2019)* demonstrated that total column water vapor from ERA5 performance well over TP.
131 We firstly investigate the quality of evaporation and precipitation in ERA5 dataset by comparing
132 with the satellite observation and other reanalysis datasets (Figures not shown). The relatively
133 accurate evaporation data is developed by *Chen et al. (2019)*, which revised the Surface Energy
134 Balance System (SEBS) parameterization of bare soil to correct the biases of excess resistance to
135 heat transfer and has been demonstrated to perform well. The 2001-2016 monthly mean
136 evaporation from ERA5 is highly correlated with the satellite observations, with correlation
137 coefficient reaching 0.88 and mean absolute deviation of 13.0 mm. Furthermore, the
138 precipitation from ERA5, ERA-interim, Global Precipitation Climatology Project (GPCP, *Adler*
139 *et al., 2003*) version 2.3 and Climatic Research Unit (CRU, *Harris et al., 2020*) TS version 4.03
140 have been compared with that from the High Asia Reanalysis (HAR, *Maussion et al., 2014*),
141 which is recognized good performance over the TP (*Li et al., 2020*). Among those datasets,
142 monthly precipitation of ERA5 shows smallest bias of -5.4 mm and highest correlation
143 coefficient of 0.97.

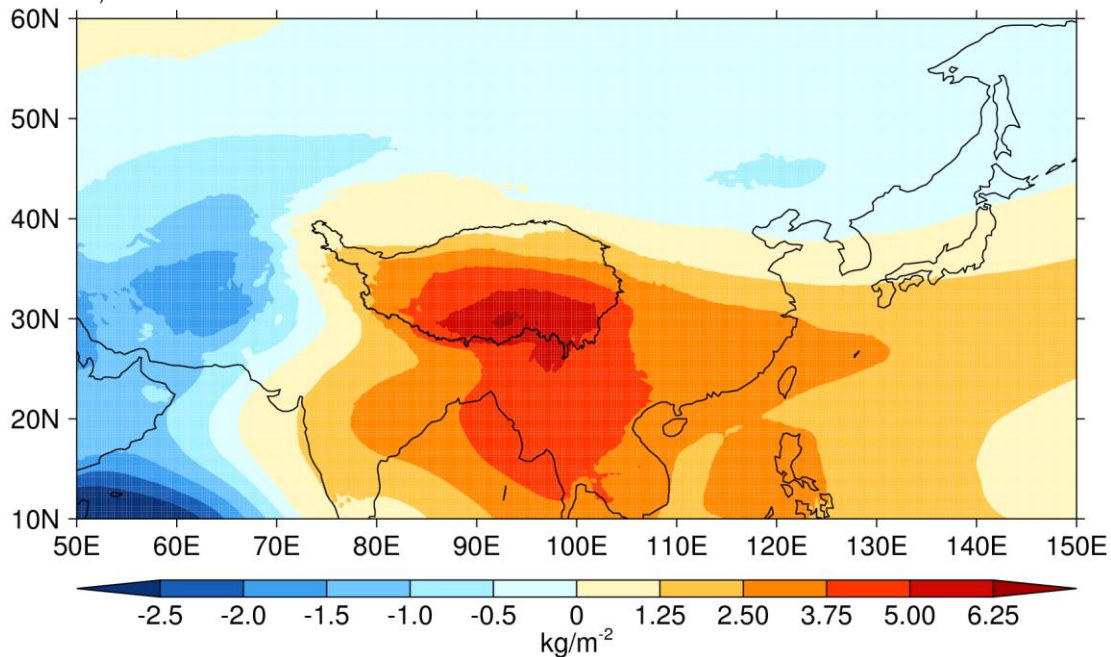
144 **3 Results**

145 3.1 Climatology/Feature of Atmospheric Water Tower

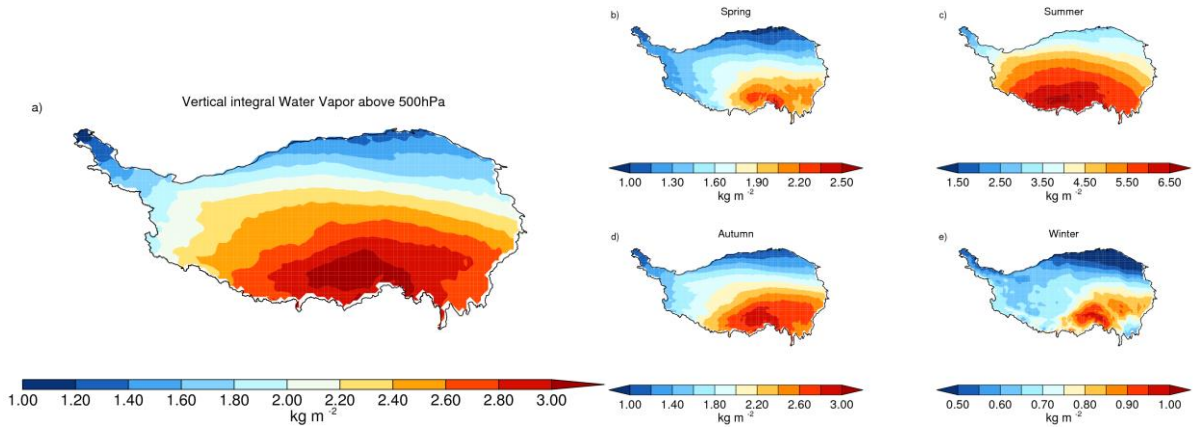
146 Based on the ERA5 40-year (1979-2018) monthly reanalysis, considering about the average
 147 elevation of the TP over 4000 m, we use specific humidity vertically integrated from 500 hPa to
 148 the top of atmosphere to represent the atmospheric water resources over the TP:

$$149 \quad w = -\frac{1}{g} \int_{500}^1 q \, dp,$$

150 where g is gravitational acceleration, q is specific humidity in unit of kg kg^{-1} , p is pressure level,
 151 and w is vertically integral specific humidity in unit of kg/m^2 , which is equivalent to millimeter.
 152 Figure 1 show the zonal deviation of annual mean vertically integral specific humidity and the
 153 black thick line shows the shape of the TP. Compared with the same latitude zone, a maximum
 154 of moisture exists right above the southern TP and south of the Himalayan region in the middle
 155 and upper stratosphere. Such a long-term existed wet pool in high atmospheric layer presents an
 156 image of atmospheric water tower (AWT). Formation of this AWT is due to the elevated terrain
 157 of the TP, which acts as a heat source and pumps water vapor from low-levels of Arabian Sea and
 158 Indian Ocean to high-levels of TP. And higher altitude helps water vapor transport farer and
 159 presents a “re-channel function” in planetary-scale (*Xu et al., 2008a*).



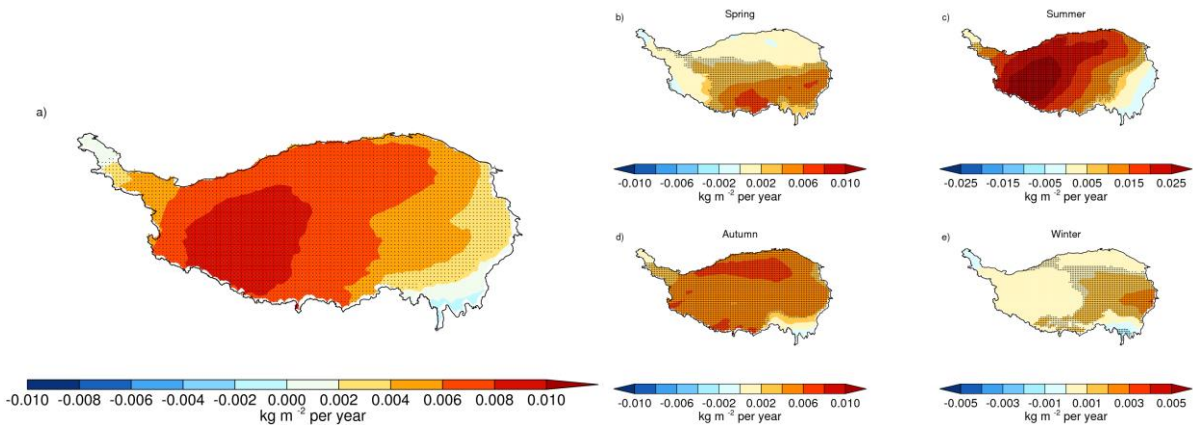
160 **Figure 1.** The zonal deviation of 40-year (1979-2018) annual mean water vapor content vertically integrated from
 161 500 to the top of the atmosphere.
 162



163

164 **Figure 2.** The horizontal distribution of 40-year (1979-2018) averaged water vapor content vertically integrated
 165 above 500 over Tibet Plateau for (a) annual, (b) spring, (c) summer, (d) autumn, and (e) winter.

166 Take a look at the long-term annual mean and seasonal mean distribution of vertically
 167 integral specific humidity above 500 hPa over the TP in (Figure 2), its general characteristics is
 168 wet in southern and southeastern TP and dry in northwestern and northeastern TP. Yarlung
 169 Zangbo Grand Canyon and relatively lower elevation in southeastern TP provide more chance
 170 for the warm and humid airflow from the oceans or seas to climb up the south slope of the TP
 171 and come into the inner land. Meanwhile, the polar dry air is blocked on the north side of the TP
 172 and water vapor from south is difficult to transport to the north. These processes lead to the
 173 extreme dry climate in the north side of the TP. The central location and magnitude of maximal
 174 moisture show significant annual variation. In winter, the wettest center is located in the
 175 southeast of TP with peak value of vertically integral specific humidity less than 1 kg/m^2 . As
 176 spring coming, the maximum center spreads to north and west with the peak value up to 3 kg/m^2 .
 177 In summer, wet regions occupy the entire southern TP with the maximum value close to 7 kg/m^2 ,
 178 then this wet regions shrink back to southeast of the TP along with autumn coming. This annual
 179 variation indicates that the atmospheric water resource over the TP is strongly influenced by
 180 South Asian monsoon and East Asian monsoon. As the outbreak of the summer Asian monsoon,
 181 wet areas expand and moisture in atmosphere increases.



182

183 **Figure 3.** The horizontal distribution of long-term (1979-2018) trends of above 500 hPa vertical integral water vapor
 184 content over Tibet Plateau for (a) annual, (b) spring, (c) summer, (d) autumn, and (e) winter

185 In the past few decades, the increase rate of air temperature in the TP is almost two times
 186 higher than that in the global (*Chen et al., 2014*). It would accelerate the melting of glaciers and

187 snow. Since atmospheric water resource is an important supply to surface water resources, long-
 188 term trends of atmospheric water resource over the TP should be concerned. Figure 3 shows the
 189 horizontal distribution of long-term trends of vertically integral specific humidity above 500 hPa
 190 over the TP for annual mean (Figure 3a) and four seasons (Figure 3b-e), respectively. The black
 191 dot means that the trend in corresponding grid is confidence in 95% level. From 1979 to 2018,
 192 except the wettest region in southeastern TP, the atmospheric water resources across the main
 193 body of the TP show significant growth trends. The trends distribution in summer has similar
 194 pattern with the overall long-term trends but larger values. For other three seasons, long-term
 195 trends are all increase but smaller than that in summer. It suggests that these upward trends are
 196 mainly contributed by changes of atmospheric circulation and heat sources in summer. The inner
 197 TP, where is relative dry condition, is the most wetting region, while the southeastern TP, the
 198 wettest climatology, become slightly dry. As *Xu and Gao (2019)* explained that decrease trends
 199 in southeastern TP is due to the less water vapor transportation from Indian Ocean.

200 3.2 Atmospheric Water Balance over TP

201 Previous researches have pointed out that there are many impactors for the changes of water
 202 vapor over TP, such as atmospheric circulation, temperature, elevation and land surface process
 203 (eg., *Duan et al., 2018; Zhou et al., 2019; Xu & Gao, 2019*). Therefore, analyses referring to
 204 water vapor budget are employed to investigate long-term trends of water vapor convergence,
 205 evaporation and precipitation across the TP (Fig. 6) as those used in many previous studies
 206 (*Chou & Neelin, 2004; Zhou et al., 2019*). The moisture budget equation is expressed as,

$$207 \quad \frac{\partial w}{\partial t} = -\nabla \cdot Q + E - P + res \quad (1)$$

208 where w is vertically integrated atmospheric water vapor, P and E are precipitation and
 209 evaporation, respectively. $\frac{\partial w}{\partial t}$ is the time derivative of vertically integrated moisture, $-\nabla \cdot Q$ is
 210 horizontal divergence of water vapor and res is the residual term, which is possible related to the
 211 assimilation in the reanalysis dataset. Comparing with other terms in Eq.(1), $\frac{\partial w}{\partial t}$ is much
 212 smaller and typically neglected, however, it also determines the trend of atmospheric water vapor
 213 over the TP. To investigate the mechanism of long-term variation of atmospheric water tower
 214 over the TP under global warming, the horizontal net water vapor flux, evaporation and
 215 precipitation were examined individually.

216 3.2.1 Horizontal Net Water Vapor Flux over the TP

217 Based on Green's theorem that the sum of fluid outflowing from a volume is equal to the total
 218 outflow summed about an enclosing area, there are following two methods (Equation (5) and (6))
 219 to achieve the horizontal net water vapor flux over the TP.

$$220 \quad IQU = \int_{sfc}^{toa} \frac{qu}{g} dp \quad (2)$$

$$221 \quad IQV = \int_{sfc}^{toa} \frac{qv}{g} dp \quad (3)$$

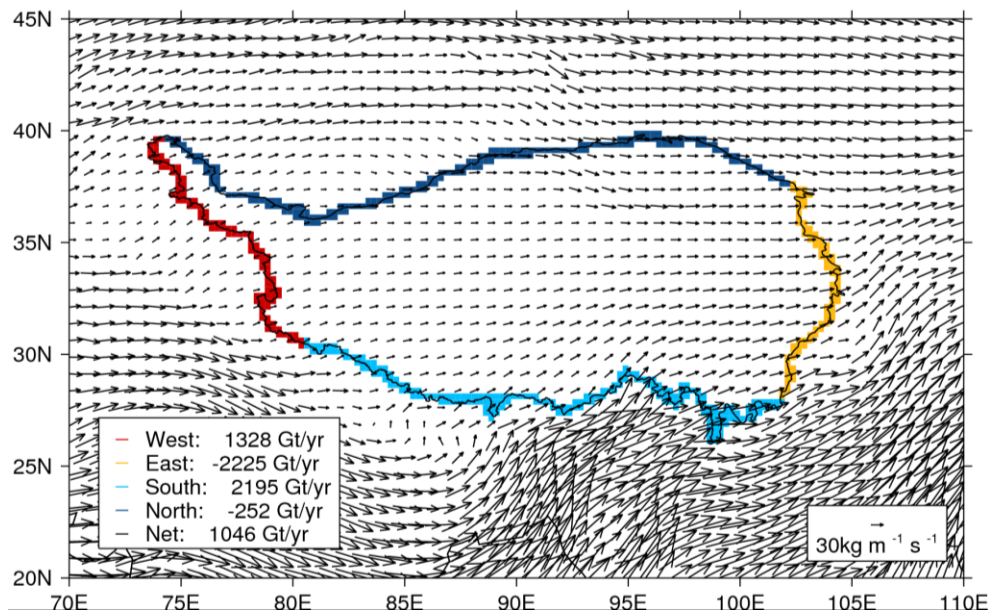
$$222 \quad D = \frac{\partial IQU}{\partial x} + \frac{\partial IQV}{\partial y} \quad (4)$$

$$N = \oint_{tp} IQUdy + IQVdx \quad (5)$$

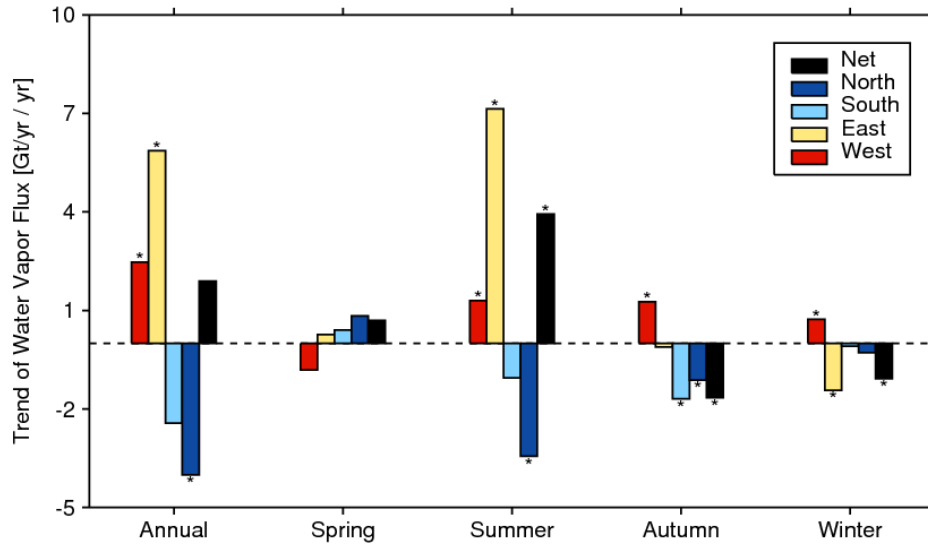
$$N = \iint_{tp} D d\sigma \quad (6)$$

225 where q is specific humidity, u and v are wind speeds in eastward and northward, respectively.
 226 IQU and IQV are respective eastward and northward water vapor flux. D is the divergence of
 227 vertical integrated water vapor flux, this parameter is positive for moisture spreading out, and
 228 negative for moisture concentrating or converging. σ is the area in unit of km^2 . N is the net
 229 income of atmospheric water resource for the entire area of the TP and the unit is Gt.

230 Based on Equation (5) and the climatology (1979-2018) from the ERA5 dataset, the vertical
 231 integral of water vapor flux in the four boundaries over the TP were shown Figure 4. The
 232 western, southern, eastern and northern boundaries are given in red, light blue, yellow and navy
 233 blue, respectively. The result shows that the water vapor over the TP was transported from
 234 western and southern boundaries with water vapor flux of 1328 Gt /a and 2195 Gt /a,
 235 respectively. And water vapor flows out in the eastern and northern boundaries with flux of -
 236 2225 Gt /a and -252 Gt /a, which are consistent with previous study based on ERA-interim ([Zhou](#)
 237 [et al., 2019](#)). Therefore, the atmospheric water tower is mainly influenced by the water vapor
 238 transported from the west and south of the TP, which are associated with the interaction between
 239 westerly and monsoon system ([Yao et al., 2019](#)). [Xu et al. \(2002, 2019\)](#) provided a conceptual
 240 model of the key influence area of water vapor transport “large triangle sector” in the TP and
 241 low-latitude ocean monsoon region. This model considers the TP as a transfer station drawing
 242 water vapor from Indian Ocean and transferring to downstream. As the water vapor pumping in
 243 the TP, 1046 Gt of water vapor in every year are left to form precipitation or increase
 244 atmospheric water vapor content.



245
 246 **Figure 4.** Vertical integral of water vapour flux from ERA-Interim (1979-2018) over the Qinghai-Tibet Plateau,
 247 whose northern, western, southern and eastern boundary are show in colors.



248

249

250 **Figure 5.** The long-term (1979-2018) of the net water vapor flux for north (deep blue), south (light blue), east
 251 (yellow), west boundary (red) of Qinghai-Tibet Plateau and net flux (black) respective in spring, summer, autumn,

252

253

254

255

256

257

258

259

260

261

262

263

264

265

266

267

268

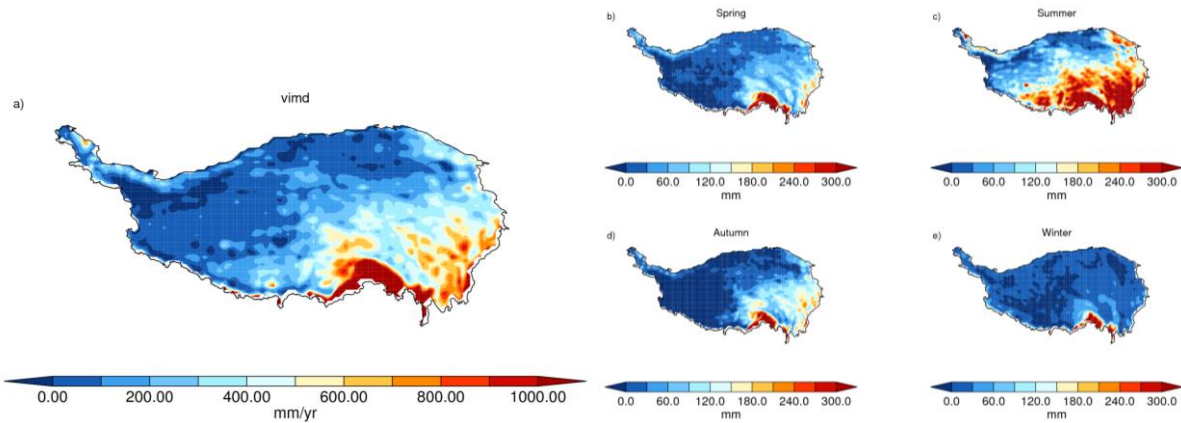
269

270

271

272

Long-term trends of the net water vapor flux over the TP region and accumulated water vapor flux passing through four boundaries are further investigated (Figure 5). Stars marked on each histogram mean that the trend is significant in 0.05. The annual mean of net water vapor flux over the TP was slightly increasing by 1.9 Gt/a, which is dominated by the trend of summer. Results showed that the increasing trend of atmospheric water tower was induced by the increasing inflow transportation from western boundaries and the decreasing outflow transportation in the eastern boundary. However, the decreasing inflow transportation from southern boundary and increasing outflow transportation from northern boundary were negatively contributed to the increasing trend of net water vapor flux over the TP. By analyzing the seasonal transportation in four boundaries, we found that the net water flux over the TP were significant increasing in summer but slightly decreasing in autumn and winter. And trends of water vapor flux in four boundaries changed dramatically in summer but lightly in other three seasons. Although the west and south boundaries are main water vapor channels in the climatology, trends of water flux in western and southern boundaries were not larger than that in eastern and northern boundaries, especially in summer. It suggested that increasing of the net water vapor flux over TP may be not induced by the interaction between westerly and monsoon system. The water vapor flux of northern boundary in summer and annual mean were significantly decreasing, which may be related to the northward shift of subtropical westerly jet (*Lin et al., 2013*) and cyclonic anomalous near Lake Baikal (*Zhou et al., 2019*). The decreasing of water flux in east boundary contributes most to the trend of the net water vapor flux and may be associated with the weakening of wind speed over the TP (*Lin et al., 2013*).



273

274 **Figure 6.** The horizontal distribution of 40-year (1979-2018) averaged vertical integrated divergence of water vapor
 275 flux over Tibet Plateau for (a) annual, (b) spring, (c) summer, (d) autumn, and (e) winter.

276

277

278

279

280

281

282

283

284

285

286

287

288

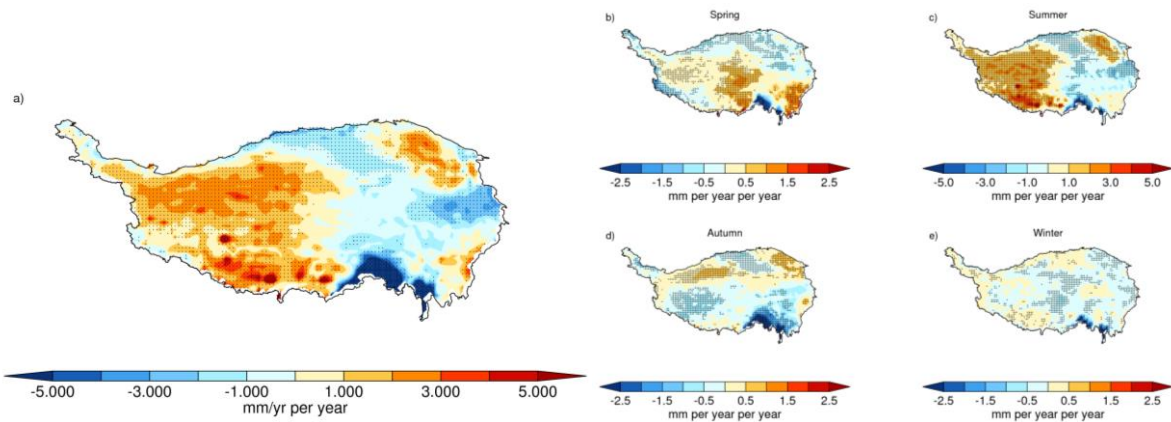
289

290

291

292

Based on Equation (4), the long-term annual and seasonal mean distribution of divergence of vertically integrated water vapor flux (D) over the TP are given in Figure 6. It means moisture spreading out (converging) when the value of D is positive (negative). Except for a few places in northwest of the TP, water vapor flux is converging for most area of the TP with weak convergences of less than 100 mm every year in western and northern TP as well as strong convergences up to 4000 mm every year in south slope and southeast of the TP. The highest converging center, which is along with Yarlung Zangbo Grand Canyon, has been recognized as the major passageway for water vapor entering the TP (*Xu et al., 2002*). The distribution of divergence of water vapor flux showed significant seasonal variation. In winter, the converging center of water vapor flux is located at the Nyingchi with maximum value about 300 mm but even diverging over the rest area of the TP. In spring and autumn, the converging center expanded to southeast of the TP. As summer coming, water vapor converging region occupies the entire TP and almost half area of the TP with divergence of water vapor flux exceeding 300 mm. Seasonal variation indicates that the atmospheric water vapor transportation over the TP is strongly influenced by South Asian monsoon and East Asian monsoon and the topography of the TP. Based on Equation (6), the net income of atmospheric water vapor for the entire TP is 1103.6 Gt, which is close to that (1046 Gt) calculated by Equation (5).



293

294

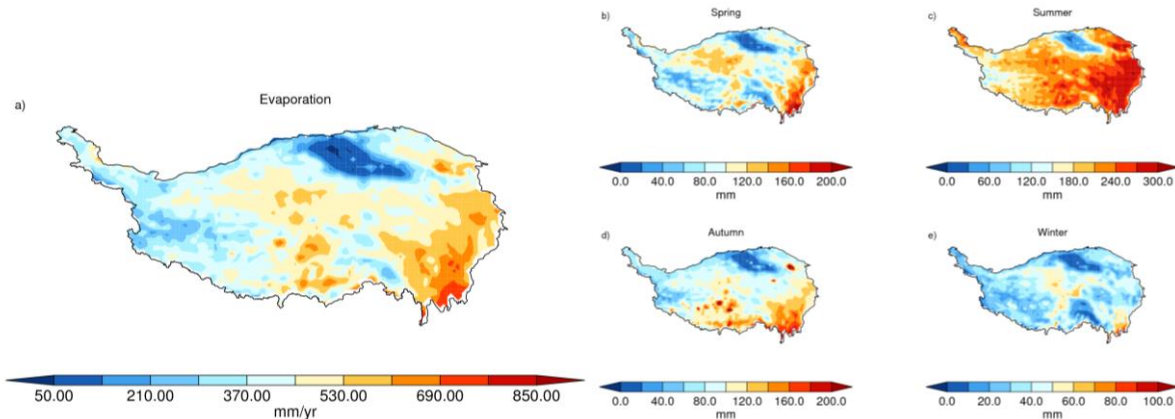
295

Figure 7. The horizontal distribution of long-term (1979-2018) trends of vertical integrated divergence of water
 vapor flux over Tibet Plateau for (a) annual, (b) spring, (c) summer, (d) autumn, and (e) winter

296 Divergence of vertically integrated water vapor flux showed dramatically decrease trends in
297 the highest converging center located at the Yarlung Zangbo Grand Canyon and slightly decrease
298 trends in the Qaidam Basin and the east of the TP. For weak converging area, such as the Qilian
299 Mountain and the inner TP, long-term trends of divergence of water vapor flux showed
300 significant upward trends (Figure 7). For different seasons, long-term trends keep decreasing at
301 the Yarlung Zangbo Grand Canyon. The distribution of long-term trends of water vapor
302 divergence in summer is similar with annual mean and trends are much larger than that in other
303 three seasons. *Duan et al. (2018)* found that the heat of the TP showed a weakening trend since
304 the 1980s based on site observations, while *Luo et al. (2019)* obtained the opposite trend of
305 plateau heat sources based on reanalysis data. As the observation sites are mainly distributed in
306 the southeast of the plateau but the sites in the middle and northwest of the plateau are seriously
307 missing, changes of heat sources from observations is contrary to those from the reanalysis data.
308 Therefore, the long-term trends of divergence of water vapor flux and heat sources show similar
309 patterns that the southeast side shows a cooling and drying trend, and the central and
310 northwestern parts show a warming and moistening tendency. It reveals that moisture
311 convergence are dominated by atmospheric heat source. *Ma et al. (2017)* also speculate that the
312 weakening water vapor transportation in southeast of TP is due to wind stilling. Besides those
313 reasons, less water vapor transportation from Indian Ocean might be another reason to the
314 decrease trend in southeastern TP (*Xu & Gao, 2019*). On the other side, the increasing
315 atmospheric water content would absorb more long-wave radiation and intensify the apparent
316 heating source, which could strengthen the convergence of water vapor and form a positive
317 feedback. While the *Yang et al. (2011b)* point out the water vapor increasing might lead to solar
318 diming over the TP. Thus, the feedback of increasing water vapor to heat source need to be
319 resolved in the future.

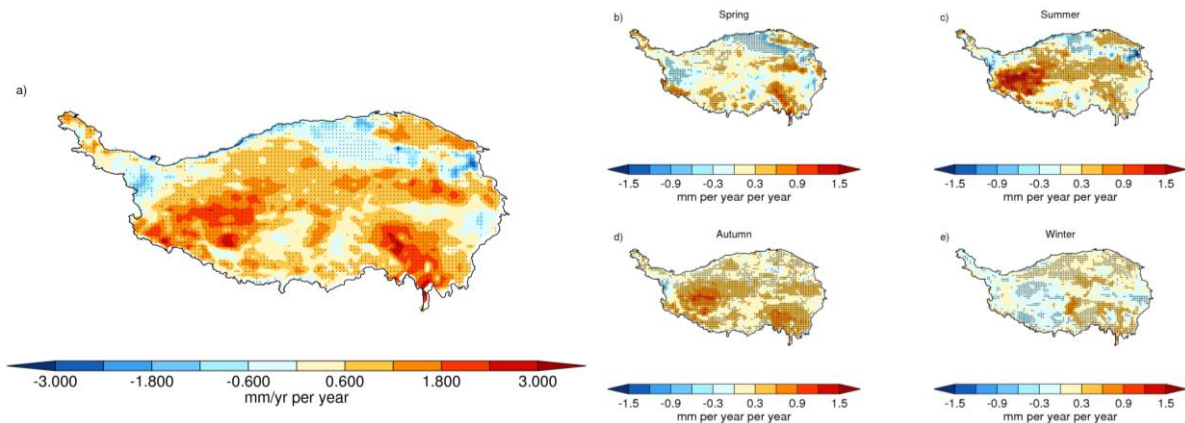
320 3.2.2 Evaporation over the TP

321 To estimate the total evaporation over the TP, we use the sum of evaporation and snow
322 evaporation from ERA5 in Figure 8. Annual accumulated total evaporations are up to 800 mm/a
323 in southeast of TP but drop to 100 mm/a in west and northwest of TP. Ranges of evaporations
324 are almost same as that of divergence of water vapor flux in most areas of the TP. As most of the
325 lakes in the TP scattered over the inner TP, evaporation is relative higher in this region. The
326 lowest evaporation (< 100 mm/a) is located at the Qaidam Basin, where is the driest area of the
327 TP. The locations of maximal and minimal evaporation did not change from season to season,
328 while the magnitude of total evaporation show significant seasonal variations due to the changes
329 of air temperature. During summer, areas with evaporation over 200 mm take part of about 80%
330 of the TP. In spring and autumn, the value of evaporation is about two third of that in summer
331 but two times of that in winter.



332

333 **Figure 8.** The horizontal distribution of 40-year (1979-2018) averaged evaporation over Tibet Plateau for (a) annual,
 334 (b) spring, (c) summer, (d) autumn, and (e) winter.



335

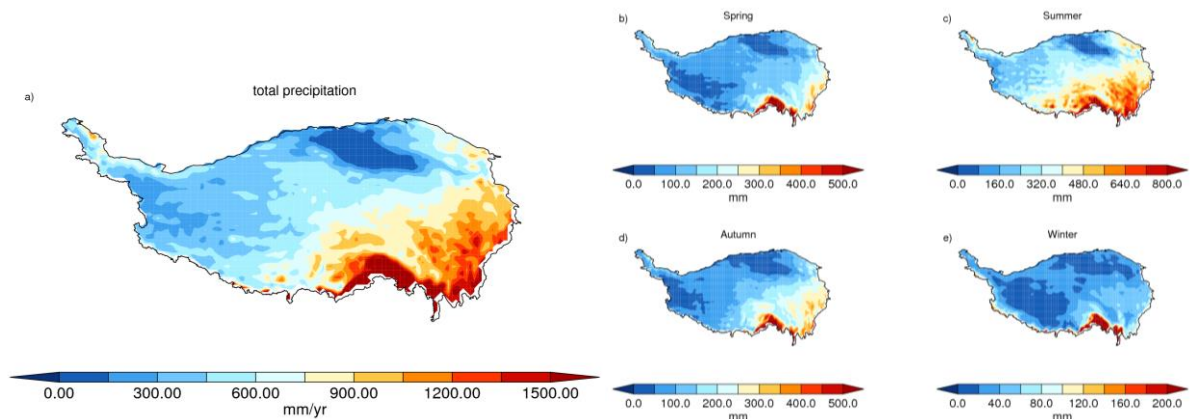
336 **Figure 9.** The horizontal distribution of long-term (1979-2018) trends of evaporation over Tibet Plateau for (a)
 337 annual, (b) spring, (c) summer, (d) autumn, and (e) winter.

338 Total evaporation shows significant increasing trends for the most part of places over the TP,
 339 except for a few of places, such as the Qaidam Basin and Karakorum Mountains (Figure 9). In
 340 general, it is consistent with the independent modeling study (*Yin et al., 2013*) and site
 341 observations (*Zhang et al., 2007; Yang et al., 2014*). As the TP has experienced enhanced
 342 temperature increase, glaciers melting and lake expansion in the past few decades (*Yao et al.,*
 343 *2019*), increase in evaporation is consistent with expectation. Based on the characteristic of seasonal
 344 variation, regions with increasing evaporation can be divided into two categories. One is located
 345 in the western and inner TP, which shows significant seasonal variation that notable increase in
 346 summer and autumn, slightly increase in spring but decrease in winter. Another one is located in
 347 the southeastern TP, where evaporations keep increasing for the whole year with very small
 348 seasonal variations. Impacts for actual evaporation includes the water availability at the surface,
 349 temperature gradient between air and surface and wind speed. As the latter two impactors
 350 dominate the evaporation in wet area, increase in evaporation in the southeast of the TP is mainly
 351 due to increase in air temperature. However, increase in evaporation in the western and inner TP
 352 is the result of the increases in both temperature and water availability at the surface. Based on
 353 Gravity Recovery and Climate Experiment (GRACE) data, *Deng et al. (2018)* found that
 354 terrestrial water storages were decreasing in the southern TP but increasing in the Inner TP from
 355 2002 to 2016. Meanwhile, based on ground survey and high-spatial-resolution satellite images,

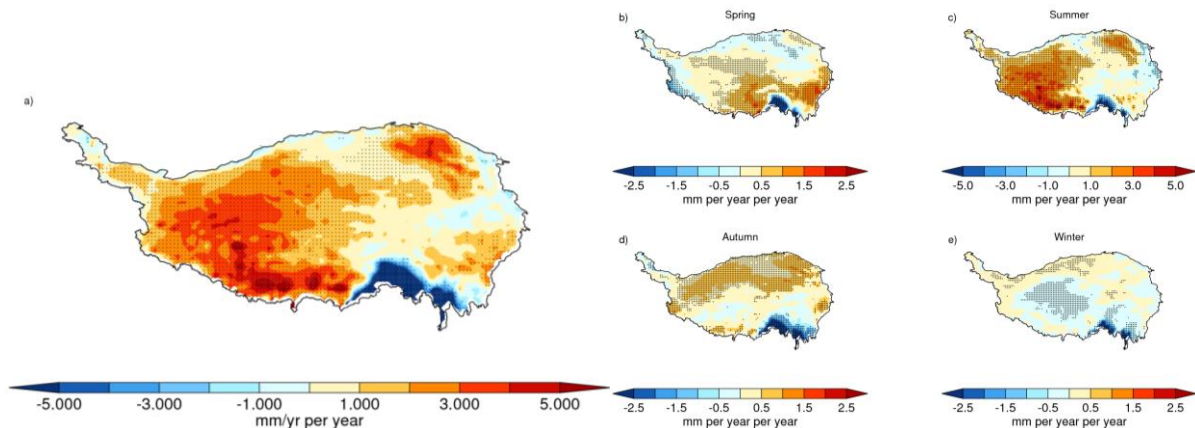
356 *Wan et al. (2016)* established a lake data set from 2004 to 2015 for the TP and found the area of
 357 lakes mainly increased in the inner TP but decrease in the Brahmaputra basin. This suggests that
 358 a consistent trend between the evaporation and water availability at the surface.

359 3.2.3 Precipitation over the TP

360 Both water vapor flux divergence and total evaporation make up of atmospheric water vapor
 361 resources to form precipitation. Figure 10 shows the horizontal distribution of 40-year (1979-
 362 2018) annual accumulated total precipitation in annual (Figure 10a) and four seasons (Figure
 363 10b-e). The distribution of precipitation combines characteristics from both divergence of water
 364 vapor flux and evaporation. The place of largest precipitation (>1500 mm/a) coincides with the
 365 largest converging center located around the Yarlung Zangbo Grand Canyon. And the least
 366 precipitation (< 150 mm/a) in the Qaidam Basin is also coexist with the place of the least
 367 evaporation. For the inner TP, relative low water vapor convergences (about 300 mm/a)
 368 combined with plentiful evaporations (about 500 mm/a) lead to considerable precipitation (about
 369 600 mm/a). Distributions of precipitation in four seasons are similar as that of the annual mean,
 370 while the magnitude of precipitation also show significant seasonal variations. The total
 371 precipitation is largest in summer, middle in spring and autumn, and smallest in winter.



372
 373 **Figure 10.** The horizontal distribution of 40-year (1979-2018) averaged total precipitation over Tibet Plateau for (a)
 374 annual, (b) spring, (c) summer, (d) autumn, and (e) winter



375
 376 **Figure 11.** The horizontal distribution of long-term (1979-2018) trends of total precipitation over Tibet Plateau for
 377 (a) annual, (b) spring, (c) summer, (d) autumn, and (e) winter.

378 Features of long-term trends of total precipitation also combines the characteristics of trends
379 of water vapor convergence and evaporation (Figure 11). Total precipitations present overall
380 long-term increasing trends for the most areas of the TP except for the Yarlung Zangbo Grand
381 Canyon, where is the region with the maximum of water vapor convergence and also the most
382 rapid decreasing of water vapor convergence. Same as the long-term trends of vertical integrated
383 divergence of water vapor flux, total precipitation keeps going down around Yarlung Zangbo
384 Grand Canyon during the whole year. It suggests that water vapor convergence related to
385 atmospheric circulation dominate the changes of precipitation in this area. Generally, the
386 locations of increasing centers of precipitation changes from season to season. The pattern of
387 long-term trends in summer is very close to that of the annual mean. In spring, precipitation
388 increase in south of the TP and decrease in north of the TP, while this pattern reverse in autumn.
389 In winter, long-term trends of precipitation are very tiny. For Brahmaputra basin, inner TP and
390 south of Qilian Mountain, increases in both water vapor flux convergence and total evaporation
391 bring about obvious increase in total precipitation. According to the values of long-term trends,
392 evaporation plays a relative important role in the increasing of precipitation in the inner TP,
393 while water vapor convergence dominates in Brahmaputra basin and south of Qilian Mountain.
394 For the source region of the Yangtze River, Yellow River and Lancang River located at the
395 center of eastern TP, overlaps of the decrease in water vapor convergence and increase in
396 evaporations give rise to no significant changes of total precipitations. As the source region of
397 three rivers supply adequate freshwater to downstream areas to feed about 40% of the world's
398 population, changeless in precipitation amount and increase in evaporation will lead to decrease
399 in surface water storage, which might be a warning alarm to us.

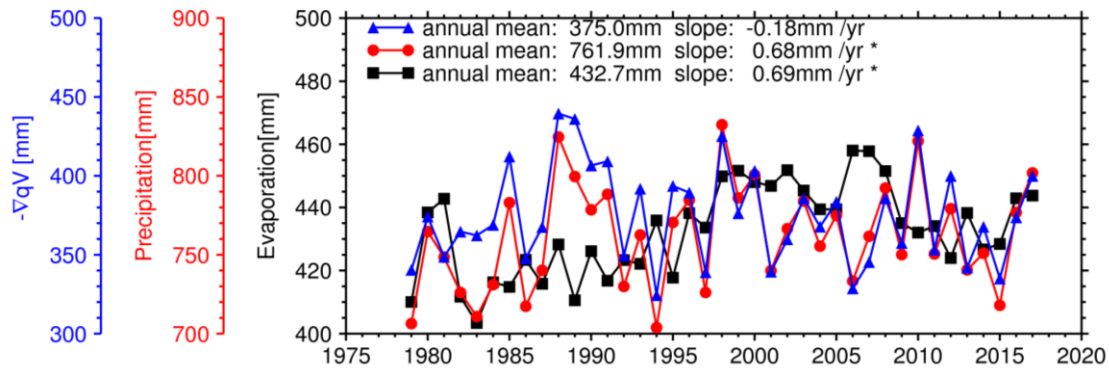
400 3.2.4 Discussion of Atmospheric Water Balance over the TP

401 Long-term means and trends of the terms in Eq. (1) are summarized in Table 1. The annual
402 vertically integrated moisture over the TP is only 15.02 Gt, which is much less than precipitation,
403 evaporation and vertical integrated water vapor convergence. This result suggests that moisture
404 converged from surround regions and/or evaporated from surface mostly leave atmosphere
405 through precipitation, only very small percent of water could be left in the atmosphere. Annual
406 accumulated precipitation is 2220.0 Gt, which is slightly less than the sum of convergence of
407 moisture (1103.6 Gt) and evaporation (1245.5 Gt). It means that atmospheric water budget
408 almost keeps equilibrium. Coincidentally, total column water (TCW) rises steadily at the rate of
409 0.011 mm/a. Precipitation over the TP is also increasing at the rate of 0.68 mm/a, which is
410 slightly less than the trend of evaporation (0.69 mm/a). However, the trend of convergence of
411 moisture decreases at the rate of -0.18 mm/a, which is not significant at 0.05 probability level.
412 Generally, changes in convergence of water vapor are caused by the changes in atmospheric
413 circulation, and more evaporation are due to expansion of the lake area and melting of glaciers
414 over the TP. Therefore, evaporation provide atmospheric water vapor locally, while the
415 divergence of water vapor flux are mainly the water transported from outside of the TP. If the
416 decrease trend of water vapor convergence turns to significant and continues, the water storage
417 of TP will be slowly depleted in the further. However, when we just check trends in summer, all
418 of the terms in Eq. (1) show increasing tendency. It suggests that increasing in both water vapor
419 convergence and evaporation brings about increasing in precipitation, and convergence of water
420 vapor (0.3 mm/a) contributes more than evaporation (0.18 mm/a). We can speculate that the
421 long-term trends of water storage in the TP is increasing in summer, which is the largest
422 atmospheric water obtain season.

423

Table 1. Atmospheric Water Budgets over the TP

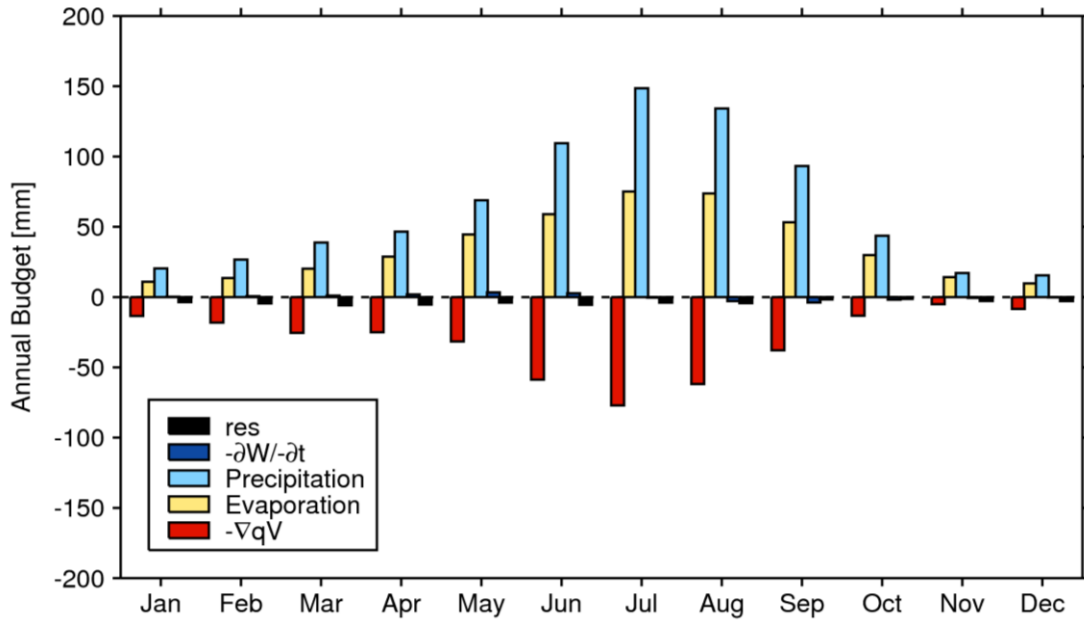
Properties		Regional [Gt]	Annual Mean [mm/m ²]	Trend (1979-2018) [mm/a]	Trend in JJA (1979-2018) [mm/a]
TCW	Status	16.10	5.16	0.011	0.030
∂W	Accumulated	0.009	0.003	0.000	0.003
$-\nabla(\mathbf{q}\vec{V})$	Accumulated	1103.6	375.0	-0.18	0.30*
E	Accumulated	1245.5	432.7	0.69*	0.18*
P	Accumulated	2220.0	761.9	0.68*	0.76*

424 *Note.* * means the trend is significant in 95% confident level.

425

426 **Figure 12.** The time series (1979-2018) of annual vertical integrated divergence of water vapor flux (blue), total
427 precipitation (red) and total evaporation (black) over the Tibet Plateau.

428 To further investigate the long-term variation of moisture balance over the TP, time series of
429 annual total evaporation, precipitation and convergence of water vapor were shown in Figure 12.
430 Results suggest that the variation of annual total precipitation is closely matched with that of
431 convergence of water vapor over the TP, while their long-term trends are different. It means the
432 water vapor convergence generally dominate the precipitation across the TP and evaporation just
433 play an assistant role. Evaporation has an obvious decadal transition from an increasing period
434 (1985-2005) to a decreasing period (2005-2015). Different with warming hiatus phenomenon in
435 globe and China, the temperature over the TP keeps same warming rate during warming hiatus
436 period (1998-2014) (*Duan et al., 2015*). The trend analysis based on the observation found that
437 decreasing net radiation and wind speed contribute to the decreasing of evaporation in recent
438 decades (*Zhang, et al., 2018*). Convergence of water vapor do not show such a decadal transition,
439 and influence by more complex changes of atmospheric circulations, such as transportation from
440 Indian Ocean (*Xu & Gao, 2019*) and cyclonic anomaly near Lake Baikal (*Zhou et al., 2019*).



441

442 **Figure 13.** Climatology (1979-2018) of annual variation of $\frac{\partial w}{\partial t}$ (deep blue), precipitation (light blue), evaporation
 443 (yellow) and vertical integrated divergence of water vapor flux (red) and residual (black).

444 Figure 13 presents the monthly climatology of the precipitation, evaporation and
 445 convergence of water vapor. Divergence of water vapor flux, evaporation and precipitation show
 446 one-peak seasonal variation with strong in summer and weak in winter. Precipitation
 447 overwhelms evaporation in the warm half year and just slightly exceeds evaporation in the cold
 448 half year. It suggests that gross surface water budget in the TP is gaining. The residuals of the
 449 water vapor balance should include phase transformation of water vapor and cross-tropopause
 450 mass exchange, both of which are tiny (*Tian et al., 2014*) in theory. Negative value of residual
 451 means that more resources of water vapor are left in atmosphere and positive value means
 452 opposite, that more moisture are removed from atmosphere by precipitation. Herein, the
 453 monthly-accumulated residual term with small negative number can be neglected.

454 4 Conclusions

455 The Tibetan Plateau (TP) is known as the "Asian Water Tower" (*Yao et al., 2012*), acts as a
 456 "heat pump" to converge water vapor from the surrounding oceans to plateau region. Combined
 457 with the contribution of the local evaporation, TP forms an isolated region of humidity in the
 458 atmosphere (*Wu et al., 2007; Xu et al., 2008*). It can be called as "Atmospheric Water Tower
 459 (AWT)" of the plateau. Based on ERA5 reanalysis data from 1979 to 2018, general
 460 characteristics of AWT shows slightly drying trends in southern and southeastern TP, where is
 461 the most wetting region of the TP, but huge wetting trends in northwest, northeast and hinterland
 462 of the TP, where are relative dry region of the TP.

463 To reply the question that whether water vapor supply could alleviate the depletion of
 464 surface water storage caused by the melting of glaciers and the increase of runoff under rapid
 465 warming, we analyses long-term trends of water vapor budgets including items of water vapor
 466 transportation, evaporation and precipitation over the TP. Annual accumulated precipitation

467 (2220.0 Gt) across the TP is almost equivalent to the sum of convergence of moisture (1103.6
468 Gt) and evaporation (1245.5 Gt). Although the long-term trend of total precipitation seems
469 increase at the rate of 0.68 mm/a, the surface water storage would not be well replenished
470 because that the evaporation increase at the rate of 0.69 mm/a and the net gain of water vapor
471 transportation do not show significant long-term changes based on two independent methods:
472 one is the integration of water vapor flux along the boundary of the TP and another is integration
473 of divergence of water vapor flux over the enclosing area of the TP. However, in summer, the
474 largest water obtain season, the trend of convergence of water vapor flux significantly increases
475 at the rate of 0.3 mm/a, which was induced by the increasing inflow transportation from western
476 boundaries and the decreasing outflow transportation in the eastern boundary. *Zhou et al. (2019)*
477 found that when a cyclonic (an anticyclonic) anomaly occurs near Lake Baikal, there is less
478 (more) water vapor over the TP, then attributed the decreasing outflow in the eastern boundary to
479 a summer atmospheric circulation anomaly near Lake Baikal.

480 For different regions of the TP, characteristic of water vapor balance and their long-term
481 trends are completely different. Regions around Yarlung Zangbo Grand Canyon, where is the
482 major passageway of water vapor transported from south oceans to TP, experiences the sharp
483 decrease in water vapor convergence and then leads to decrease in precipitation. Meanwhile, the
484 evaporation still increases due to the increasing of temperatures and melting of glaciers. Surface
485 water storage would be tremendously lost in this area. For the center of eastern TP, where is
486 source region of the Yangtze River, Yellow River and Lancang River, decrease in water vapor
487 convergence overlaps increase in evaporations leads to no significant changes in total
488 precipitations. As the evaporations provide the water vapor from local regions while water vapor
489 convergence transport water resources from the outside of the TP, it should be on the alert that
490 the water storage of this area would be slowly depleted in the further. For Brahmaputra basin,
491 inner TP and south of Qilian Mountain, there are significant wetting tendencies because that the
492 increases in both convergence of water vapor flux and evaporation bring about obvious increase
493 in total precipitation.

494 All above regional feature of water vapor balance across the TP are the result of complex
495 interaction between atmospheric heat source (*Yang et al., 2014*), atmospheric circulation from
496 high latitude regions, such as cyclone near the Lake Baikal (*Zhou et al., 2019*), and/or low
497 latitude regions, such as monsoon from the Indian Ocean (*Xu & Gao, 2019*). Meanwhile, *Liu et*
498 *al. (2019)* found that the slow increasing of precipitation may be affected by the increasing dust
499 aerosol transported from central Asian or Taklamakan desert. This study presents a general view
500 of AWT and details about impacts of the long-term changes of atmospheric water vapor balance
501 on surface water storage across the TP. It is sure to improve our understanding about “Asia
502 Water Tower” in climate research and adaptation policy.

503 **Acknowledgments**

504 This study is supported by the Strategic Priority Research Program of the Chinese
505 Academy of Sciences (XDA2006010301). The ERA5 data are available from
506 <https://cds.climate.copernicus.eu/>

507 **References**

- 508 An, Z., Kutzbach, J. E., Prell, W. L., & Porter, S. C. (2001). Evolution of Asian monsoons and
509 phased uplift of the Himalaya-Tibetan plateau since Late Miocene times. *Nature*, 411, 62-66,
510 <https://doi.org/10.1038/35075035>.
- 511 Adler, R.F., Huffman, G.J., Chang, A., Ferraro, R., Xie, P., Janowiak, J., et al. (2003). The
512 Version 2 Global Precipitation Climatology Project (GPCP) Monthly Precipitation Analysis
513 (1979-Present). *J. Hydrometeor.*, 4, 1147-1167.
- 514 Berrisford, P., Dee, D.P., Fielding, K., Fuentes, M., Kallberg, P., Kobayashi, S., & Uppala, S.M.
515 (2009). The ERA-Interim Archive. *ERA Report Series*, No.1. ECMWF: Reading, UK.
- 516 Boos, W. R., & Kuang, Z. (2010). Dominant control of the South Asian monsoon by orographic
517 insulation versus plateau heating. *Nature*, 463, 218-223, doi:10.1038/nature08707.
- 518 Chen, D.L., Xu, B.Q., Yao, T.D., Guo, Z.T., Cui, P., Chen, F.H., et al., 2015: Assessment of
519 past, present and future environmental changes on the Tibetan Plateau. *Chin. Sci. Bull.*, 60,
520 3025–3035, <https://doi.org/10.1360/N972014-01370>. (in Chinese)
- 521 Chen, X., Massman, W. J., & Su, Z. (2019). A column canopy-air turbulent diffusion method for
522 different canopy structures. *Journal of Geophysical Research: Atmospheres*, 124, 488– 506.
523 <https://doi.org/10.1029/2018JD028883>.
- 524 Cheng, G., & Wu, T. (2007), Responses of permafrost to climate change and their
525 environmental significance, Qinghai-Tibet Plateau, *J. Geophys. Res.*, 112, F02S03,
526 doi:10.1029/2006JF000631. Chou, C., & Neelin, J. D. (2004). Mechanisms of global warming
527 impacts on regional tropical precipitation. *Journal of Climate*, 17(13), 2688-2701.
- 528 Dee, D. P., Uppala, S.M., Simmons, A.J., Berrisford, P., Poli, P., Kobayashi, S., et al. (2011).
529 The ERA-Interim reanalysis: configuration and performance of the data assimilation system.
530 *Quart. J. R. Meteorol. Soc.*, 137, 553–597.
- 531 Deng, H., Pepin, N. C., Liu, Q., & Chen, Y. (2018). Understanding the spatial differences in
532 terrestrial water storage variations in the Tibetan Plateau from 2002 to 2016, *Clim. Change*,
533 151(3–4), 379–393, doi:10.1007/s10584-018-2325-9.
- 534 Ding, Y., & Chan, J. (2005). The east Asian summer monsoon: an overview. *Meteorol. Atmos.*
535 *Phys.*, 89(1):117–142.
- 536 Duan, A., & Wu, G. (2008). Weakening trend in the atmospheric heat source over the Tibetan
537 Plateau during recent decades. Part I: observations. *J. Clim.*, 21, 3149–3164.
- 538 Duan, A., & Wu, G. (2009). Weakening trend in the atmospheric heat source over the Tibetan
539 Plateau during recent decades. Part II: connection with climate warming. *J. Clim.*, 22, 4197–
540 4212.
- 541 Duan, A., & Xiao, Z. (2015). Does the climate warming hiatus exist over the Tibetan Plateau?.
542 *Sci. Rep.*, 5, 13711. <https://doi.org/10.1038/srep13711>.
- 543 Duan, A., Liu, S., Zhao, Y., Gao, K., & Hu, W. (2018). Atmospheric heat source / sink dataset
544 over the Tibetan Plateau based on satellite and routine meteorological observations. *Big Earth*
545 *Data*, 00(00), 1–11. <https://doi.org/10.1080/20964471.2018.1514143>

- 546 Feng, L., & Zhou, T. (2012). Water vapor transport for summer precipitation over the Tibetan
547 Plateau: Multidata set analysis, *J. Geophys. Res.*, 117, D20114, doi:10.1029/2011JD017012.
- 548 Gao, L., Gou, X., Deng, Y., Wang, Z., Gu, F., Wang, F. (2018). Increased growth of Qinghai
549 spruce in northwestern China during the recent warming hiatus. *Agricultural and Forest*
550 *Meteorology*, 260–261, 9-16.
- 551 Guo, D., & Wang, H. (2012). The significant climate warming in the northern Tibetan Plateau
552 and its possible causes. *Int. J. Climatol.* 32, 1775–1781, <http://dx.doi.org/10.1002/joc.2388>.
- 553 Harris, I., Osborn, T.J., Jones, P., Lister, D. (2020). Version 4 of the CRU TS monthly high-
554 resolution gridded multivariate climate dataset. *Scientific Data*, 7, 109,
555 <https://doi.org/10.1038/s41597-020-0453-3>
- 556 Immerzeel, W.W., van Beek, L.P.H., Bierkens, M.F.P. (2010). Climate change will affect the
557 Asian water towers. *Science*, 328, 1382–1385
- 558 Li, D., Yang, K., Tang, W., Li, X., Zhou, X., & Guo, D. (2020). Characterizing precipitation in
559 high altitudes of the western Tibetan plateau with a focus on major glacier areas, *Int. J.*
560 *Climatol.*, (February), doi:10.1002/joc.6509.
- 561 Li, W., Guo, W., Qiu, B., Xue, Y., Hsu, P. C., & Wei, J. (2018). Influence of Tibetan Plateau
562 snow cover on East Asian atmospheric circulation at medium-range time scales. *Nat. Commun.*,
563 9(1), doi:10.1038/s41467-018-06762-5.
- 564 Li, W., Qiu, B., Guo, W., Zhu, Z., & Hsu, P. C. (2019). Intraseasonal variability of Tibetan
565 Plateau snow cover, *Int. J. Climatol.*, (November), doi:10.1002/joc.6407.
- 566 Lin, C., Yang, K., Qin, J., & Fu, R. (2013). Observed Coherent Trends of Surface and Upper-Air
567 Wind Speed over China since 1960. *J. Climate*, 26, 2891–2903, [https://doi.org/10.1175/JCLI-D-](https://doi.org/10.1175/JCLI-D-12-00093.1)
568 12-00093.1.
- 569 Liu, Y., Zhu, Q., Huang, J., Hua, S., & Jia, R. (2019). Impact of dust-polluted convective clouds
570 over the Tibetan Plateau on downstream precipitation. *Atmos. Environ.*, 209, 67-77. doi:
571 10.1016/j.atmosenv.2019.04.001.
- 572 Liu, X., & Chen, B. (2000). Climatic warming in the Tibetan Plateau during recent decades. *Int.*
573 *J. Climatol.*, 20, 1729–1742.
- 574 Lu, C., Yu, G., & Xie, G. (2005). Tibetan Plateau serves as a water tower. *IEEE Trans. Geosci.*
575 *Remote Sens.*, 5, 3120– 3123.
- 576 Luo, X., & Xu, J. (2019). Estimate of atmospheric heat source over Tibetan Plateau and its
577 uncertainties. *Climate Change Research*, 15(1): 33-40.(in Chinese)
- 578 Lutz, A. F., Immerzeel, W. W., Shrestha, A. B., & Bierkens, M. F. P. (2014). Consistent increase
579 in High Asia's runoff due to increasing glacier melt and precipitation, *Nat. Clim. Chang.*, 4(7),
580 587–592, doi:10.1038/nclimate2237.
- 581 Ma, Y., Ma, W., Zhong, L., Hu, Z., Li, M., Zhu, Z., Han, C., Wang, B., & Liu, X. (2017).
582 Monitoring and Modeling the Tibetan Plateau's climate system and its impact on East Asia, *Sci.*
583 *Rep.*, 7, 1–6, doi:10.1038/srep44574.

- 584 Maussion, F., Scherer, D., Mölg, T., Collier, E., Curio, J., & Finkelburg, R. (2014).
585 Precipitation Seasonality and Variability over the Tibetan Plateau as Resolved by the High Asia
586 Reanalysis. *J. Climate*, 27, 1910–1927, doi:10.1175/JCLI-D-13-00282.1.
- 587 Molnar, P., England, P., & Martinod, J. (1993). Mantle dynamics, uplift of the Tibetan Plateau,
588 and the Indian Monsoon, *Rev. Geophys.*, 31(4), 357-396, doi:10.1029/93RG02030.
- 589 Moore, G.W.K. (2012). Surface pressure record of Tibetan Plateau warming since the 1870s. *Q.*
590 *J. R. Meteorol. Soc.*, 138, 1999–2008.
- 591 Sugimoto, S., Ueno, K., Sha, W. (2008). Transportation of Water Vapor into the Tibetan Plateau
592 in the Case of a Passing Synoptic-Scale Trough. *Journal of the Meteorological Society of Japan*,
593 86(6):935-949.
- 594 Tian, H., Tian, W., Luo, J., Zhang, J., & Zhang, M. (2017). Climatology of cross-tropopause
595 mass exchange over the Tibetan Plateau and its surroundings. *Int. J. Climatol.*, 37: 3999-4014,
596 doi:10.1002/joc.4970
- 597 Ueno, K., Toyotsu, K., Bertolani, L., & Tartari, G. (2008). Stepwise onset of monsoon weather
598 observed in the Nepal Himalayas. *Mon. Weather Rev.*, 136, 2507– 2522.
- 599 Wan, W., Long, D., Hong, Y., Ma, Y., Yuan, Y., Xiao, P., et al. (2016). A lake data set for the
600 Tibetan Plateau from the 1960s, 2005, and 2014. *Sci. Data*, 3:160039 doi: 10.1038/sdata.2016.39
- 601 Wan, B., Gao, Z., Chen, F., & Lu, C. (2017). Impact of Tibetan Plateau Surface Heating on
602 Persistent Extreme Precipitation Events in Southeastern China. *Monthly Weather Review*, 145,
603 3485–3505.
- 604 Wang, Y., Xu, X., Lupo, A. R., Li, P., & Yin, Z. (2011). The remote effect of the Tibetan Plateau
605 on downstream flow in early summer. *J. Geophys. Res.*, 116, D19108,
606 doi:10.1029/2011JD015979.
- 607 Wang, Y., Yang, K., Pan, Z., Qin, J., Chen, D., Lin, C., et al. (2017). Evaluation of precipitable
608 water vapor from four satellite products and four reanalysis datasets against GPS measurements
609 on the Southern Tibetan Plateau. *J. Clim.*, 30(15), 5699–5713, doi:10.1175/JCLI-D-16-0630.1.
- 610 Wu, G., Liu, Y., He, B., Bao, Q., Duan, A., Jin, F. F. (2012a). Thermal controls on the Asian
611 summer monsoon. *Sci. Rep.*, 2, 4, <https://doi.org/10.1038/srep00404>.
- 612 Wu, G. X., Liu, Y. M., Dong, B. W., Liang, X. Y., Duan, A. M., Bao, Q., & Yu, J. J. (2012b).
613 Revisiting Asian Monsoon Formation and Change Associated with Tibetan Plateau Forcing: I.
614 Formation. *Clim. Dyn.*, 39(5), 1169-1181, doi:10.1007/s00382-012-1334-z.
- 615 Wu, G. X., Liu, Y. M., Wang, T. M., Wan, R. J., Liu, X., Li, W. P., et al. (2007). The influence
616 of mechanical and thermal forcing by the Tibetan Plateau on Asian climate, *J. Hydro. Meteor.*
617 *Spec. Sect.*, 8, 770-789, doi:10.1175/JHM609.1.
- 618 Wu, G. X., & Zhang, Y. S. (1998). Tibetan Plateau Forcing and the Timing of the Monsoon
619 Onset over South Asia and the South China Sea. *Monthly Weather Review*, 126(4):913-927.
- 620 Xu, X., Zhou, M., Chen, J., Bian, L., Zhang, G., Liu, H., et al. (2002). A comprehensive physical
621 pattern of land-air dynamic and thermal structure on the Qinghai-Xizang Plateau, *Science in*
622 *China Series D: Earth Sciences*, 45(7), 18–24.

- 623 Xu, X., Lu, C., Shi, X., & Gao, S. (2008a). World water tower: An atmospheric perspective.
624 *Geophys. Res. Lett.*, 35(20), 525-530, doi:10.1029/2008GL035867.
- 625 Xu, X. D., Shi, X. Y., Wang, Y. Q., Peng, S. Q., & Shi, X. H. (2008b). Data analysis and
626 numerical simulation of moisture source and transport associated with summer precipitation in
627 the Yangtze River Valley over China. *Meteorol. Atmos. Phys.*, 100, 217-231,
628 doi:10.1007/s00703-008-0305-8.
- 629 Xu, Y., & Gao, Y. (2019). Quantification of evaporative sources of precipitation and its changes
630 in the Southeastern Tibetan Plateau and Middle Yangtze River Basin. *Atmosphere*, 10(8).
631 <https://doi.org/10.3390/atmos10080428>.
- 632 Yang, K., Guo, X., & Wu, B. (2011a). Recent trends in surface sensible heat flux on the Tibetan
633 Plateau. *Science in China Series D: Earth Sciences*, 54, 19–28.
- 634 Yang, K., Guo, X., He, J., Qin, J., & Koike, T. (2011b). On the climatology and trend of the
635 atmospheric heat source over the Tibetan Plateau: an experiments-supported revisit. *J. Clim.*,
636 24, 1525–1541.
- 637 Yang, K., Wu, H., Qin, J., Lin, C., Tang, W., & Chen, Y. (2014). Recent climate changes over
638 the Tibetan Plateau and their impacts on energy and water cycle: A review. *Glob. Planet.*
639 *Change*, 112, 79–91, doi:10.1016/j.gloplacha.2013.12.001.
- 640 Yao T., Thompson, L., Yang, W., Yu, W., Gao, Y., Guo, X., et al. (2012). Different glacier
641 status with atmospheric circulations in Tibetan Plateau and surroundings. *Nat. Clim. Change*, 2:
642 663–667.
- 643 Yao, T. (2019). Tackling on environmental changes in Tibetan Plateau with focus on water,
644 ecosystem and adaptation. *Science Bulletin*, 64: 417
- 645 Yin, Y., Wu, S., Zhao, D., Zheng, D., & Pan, T. (2013). Modeled effects of climate change on
646 actual evapotranspiration in different eco-geographical regions in the Tibetan Plateau. *J. Geogr.*
647 *Sci.*, 23, 195–207.
- 648 Zhang, D., Huang, J., Guan, X., Chen, B., & Zhang, L. (2013). Long-term trends of precipitable
649 water and precipitation over the Tibetan Plateau derived from satellite and surface
650 measurements. *Journal of Quantitative Spectroscopy & Radiative Transfer*, 122:64-71.
- 651 Zhang, Y., Liu, C., Tang, Y., & Yang, Y. (2007). Trends in pan evaporation and reference and
652 actual evapotranspiration across the Tibetan Plateau, *J. Geophys. Res. Atmos.*, 112(12), 1–12,
653 doi:10.1029/2006JD008161.
- 654 Zhang, C., Liu, F., & Shen, Y. (2018), Attribution analysis of changing pan evaporation in the
655 Qinghai–Tibetan Plateau, China. *Int. J. Climatol*, 38, e1032-e1043, doi:10.1002/joc.5431
- 656 Zhao, Y., & Zhou, T. (2019). Asian water tower evinced in total column water vapor: a
657 comparison among multiple satellite and reanalysis data sets. *Clim. Dyn.*, 54, 231-245,
658 doi:10.1007/s00382-019-04999-4.
- 659 Zhou, C., Zhao, P., & Chen, J. (2019). The interdecadal change of summer water vapor over the
660 Tibetan Plateau and associated mechanisms. *J. Clim.*, 32, 4103–4119, doi:10.1175/JCLI-D-18-
661 0364.1.

- 662 Zhu, Y.X., Ding, Y.H., & Xu, H.G. (2008). Decadal relationship between atmospheric heat
663 source of winter and spring snow over Tibetan Plateau and rainfall in East China. *Journal of*
664 *Meteorological Research*, 65, 946–958.
- 665 Zhu, L., Xie, M., & Wu, Y. (2010). Quantitative analysis of lake area variations and the
666 influence factors from 1971 to 2004 in the Nam Co basin of the Tibetan Plateau. *Chinese Science*
667 *Bulletin*, 55, 1294–1303.